Research

Ecography 40: 1210–1220, 2017
doi: 10.1111/ecog.02461

Subject Editor: Thorsten Wiegand. Editor-in-Chief: Miguel Araújo. Accepted 23 August 2016

Edaphic properties enable facilitative and competitive interactions resulting in fairy circle formation

Michael D. Cramer, Nichole N. Barger and Walter R. Tschinkel

M. D. Cramer (michael.cramer@uct.ac.za), Dept of Biological Sciences, Univ. of Cape Town, Cape Town, South Africa. – N. N. Barger, Dept of Ecology and Evolutionary Biology, Univ. of Colorado at Boulder, Boulder, CO, USA. – W. R. Tschinkel, Dept of Biological Science, Florida State Univ., Tallahassee, FL, USA.

Millions of generally regularly spaced, roughly circular barren patches called fairy circles occur in a narrow band ca 100 km inland of the south-west African coast. These generally have conspicuously taller peripheral grasses in a shorter grass matrix. The origins of these fairy circles are controversial, but one possibility is that they are self-organizing emergent vegetation patterns that are the consequence of interplay between positive (facilitative) and negative (competitive) interactions between grasses. We hypothesized that the coarse textured sand on which fairy circles occur creates a hydraulically and nutritionally connected landscape, in which neighbouring fairy circles competitively influence each other over several metres, while providing opportunity for focusing of resources around the peripheral grasses. To test our hypotheses we conducted three main groups of analyses: 1) we measured grass biomass to assess facilitative and competitive effects of the component grasses; 2) across a region with fairy circles we measured the size and density of fairy circles and correlated that with water infiltration rates into soil; 3) we measured the capacity of soil to conduct water pulses and ^{15}N tracers. We found evidence of facilitative interactions in the periphery of the fairy circles and competitive suppression of the matrix grass proximal to the periphery. Across the region, fairy circle size was positively correlated with soil infiltration rates and negatively with precipitation. This suggests that fairy circles emerge in soils with high capacity for water flux that enables landscape hydraulic connectivity. Water- and ^{15}N-pulse experiments showed that edaphic resources were highly mobile, moving up to 7.5 m over a period of 1–3 weeks. We concluded that the evidence is consistent with an emergent vegetation pattern explanation for the origins of fairy circles and that the circles are more closely associated with a highly connective edaphic environment, rather than with particular biota.

Vegetation in dryland ecosystems is commonly organised into spatial patterns (Aguiar and Sala 1999, Lejeune et al. 1999, Couteron and Lejeune 2001, Rietkerk et al. 2002, Deblauwe et al. 2008), including bands, spots or gaps that occur in otherwise continuous vegetation (Deblauwe et al. 2011). This range of vegetation patterns is hypothesized to emerge due to the interactions between local-scale positive (i.e. facilitative) and longer-range negative (i.e. competitive) feedbacks (Lejeune et al. 1999, Couteron and Lejeune 2001). This unifying theory of vegetation patterning is supported by many mathematical models that replicate the pattern formation, albeit through differing but non-mutually exclusive mechanisms (reviewed by Borgogno et al. 2009, Meron 2012).

The competitive and facilitative interactions generating vegetation patterning are for resources that include nutrients and light, but considering the dryland context of many vegetation patterns, are likely for water (Rietkerk and van de Koppel 2008). Competitive interactions between vegetation clumps may deplete water between the clumps resulting in bare ground, whereas runoff from bare ground may be intercepted by vegetation, increasing the soil moisture in the vegetation patch and providing facilitative feedbacks within the clump (Meron 2012). Runoff may be especially important in contributing to pattern formation where both biological and physical soil crusts reduce surface infiltration of water (Eldridge et al. 2000). Transport of water towards vegetation clumps through root interception and water potential gradients also plays a role in pattern formation (Barbier et al. 2008). The interplay between these competitive and facilitative feedbacks results in greater biomass in a region of facilitation with declining biomass away from the zone of facilitation. This change in biomass has been used as a diagnostic feature of emergent vegetation pattern (Rietkerk et al. 2000).

The 'fairy circles' found in southern Africa (reviewed by van Rooyen et al. 2004) and more recently in Australia (Getzin et al. 2016) are a striking example of a vegetation pattern. Fairy circles are characterized as regularly spaced, roughly circular barren patches that occur in grasslands (referred to as the matrix) inland (ca 100 km) of the southwest African coast between southern Angola and northern South Africa and also in the Pilbara region of Australia (Getzin et al. 2016). Although the impressive regularity of the pattern has

contributed to global interest in fairy circles, this regularity is contingent on both the homogeneity of the landscape (i.e. absence of drainage lines, rocky outcrops, etc.) and the existence of a high density of fairy circles (Cramer and Barger 2013). In Namibia fairy circles are restricted to a narrow climatic regime with mean annual precipitation (MAP) of 50–150 mm and soils that are coarse textured sands (Cramer and Barger 2013) with high infiltration rates (Moll 1994). Although strikingly similar in appearance, the African and Australian fairy circles differ in a number of respects. Australian fairy circles occur in a wetter (MAP = 327 mm), but highly variable rainfall area (MAP range: 37–619 mm), and on clay-rich soils with low infiltration rates (Getzin et al. 2016). Although similar in spatial distribution and appearance, mechanisms of fairy circle formation in Namibia and Australia likely differ (Getzin et al. 2016). Following this, we restrict further discussion of this spatial pattern to the Namibian fairy circles.

The generally barren interior of Namibian fairy circles is commonly surrounded by peripheral grasses that are taller than the matrix grassland (van Rooyen et al. 2004). Although this band of taller peripheral grass around fairy circles is common, the rings do also form without the distinctive taller peripheral grasses (Tschinkel 2012). The Namibian fairy circles are dynamic with a lifespan of ca 60 yr (Tschinkel 2012) and the average size of fairy circles decreases with increasing rainfall (Cramer and Barger 2013). This and the fact that competitive interactions between grasses in an arid ecosystem are likely to be, at least partially, for water has led to the suggestion that fairy circles are an example of vegetation gap patterns that form as a result of competitive interactions between grasses (van Rooyen et al. 2004, Tschinkel 2012, 2015, Cramer and Barger 2013), similar to the formation of gaps in vegetation in Niger (Barbier et al. 2006, 2008). The regularity of fairy circle distribution in the landscape and the correlation of fairy circle size with distances apart are also consistent with the notion of plant–plant interactions as the major vegetation-patterning mechanism (Getzin et al. 2015a, b). Furthermore, mathematical models of fairy circles based on plant–plant interactions reliably reproduce fairy circle size, shape and distribution as well as the changes in fairy circles with variation in precipitation (Tlidi et al. 2008, Fernandez-Oto et al. 2014, Getzin et al. 2015a, b, 2016, Zelnik et al. 2015).

The hypothesised vegetation-patterning mechanism for fairy circle formation requires that the fairy circles are able to interact with each other over distances of up to 13 m (Getzin et al. 2015a, b). Although runoff may occasionally occur under extremely high intensity precipitation events (Cramer and Barger 2013), the sandy soils associated with fairy circles have little to no biological soil crusts and exceptionally high infiltration rates (ca 1290 mm h^{-1}; Moll 1994). Hydraulic conductance of soils is commonly assessed from surface infiltration, for which typical values are 1–5 mm h^{-1} for clay, and < 30 mm h^{-1} for sand (Brouwer et al. 1988), although higher values have been recorded (e.g. 360 mm h^{-1} for desert soil in Arizona, Lyford and Qashu 1969). The exceptionally high infiltration rates on fairy circle soils led Cramer and Barger (2013) to propose that rather than runoff, sub-surface flow of water driven by water gradients setup by deep peripheral grass roots in coarse sand may enable competition between fairy circles for resources and consequently spatial patterning. Evidence for such long-range sub-surface water flows is, however, lacking.

Apart from the exceptionally arid conditions in areas where Namibian fairy circles occur, the association with coarse textured aeolian sand also results in exceptionally low nutrient concentrations in the soil (Cramer and Barger 2013). Considering the sandy nature of the soil where fairy circles occur and the low organic carbon concentrations (ca 0.037%), it is likely that nutrients are highly mobile with water in the soil. Nutrient mass-flow is a critical mechanism for the delivery of nutrients to plant roots, especially in circumstances where soil has low binding capacity for nutrients (Cramer et al. 2009). Indeed, Cramer and Barger (2013) found that soil N concentration was inversely related to fairy circle size, distance apart and landscape occupancy. As a consequence it is likely that competitive interactions in fairy circles are not only for water, but also for nutrients.

The ecological mechanisms for the origin of fairy circles are currently contentious (Getzin et al. 2015a, b, Juergens et al. 2015). An alternate hypothesis for the origin of fairy circles to the vegetation-patterning hypothesis is that termites generate the pattern by feeding on grasses (Moll 1994, Juergens 2013, 2015, Juergens et al. 2015, Vlieghe et al. 2015). Based on the vegetation-patterning hypothesis, however, we hypothesized (Supplementary material Appendix 1, Fig. A1) that the size and density of fairy circles is linked to characteristics of the soils that enable grasses to competitively interact with each other for water and nutrients over distances exceeding the radius of the root zone, which is typically < 1 m (Cramer and Barger 2013, Juergens 2013). To test this hypothesis we measured: 1) facilitative and competitive effects on grass biomass and root density (inferred from soil respiration) between fairy circle peripheries and the matrix; 2) the variation of soil hydraulic properties with fairy circle size and density across a fairy circle landscape; 3) the hydraulic conductance of the soil by monitoring the flux of water added to the soil and the mobility of soil nutrients by measuring plant acquisition of ^{15}N from depots remote from the plants. The evidence presented provides support for competitive and facilitative interactions determining grass biomass and also provides a potential mechanism for long-range (i.e. several metres) interactions between fairy circles that determines their size and spacing.

Methods and material

Study site

Sampling was carried out in the NamibRand private nature reserve (24.949°S, 16.040°E, 1000 m elevation) during Feb–Mar in 2014 and 2015 in the pro-Namib Desert ca 110 km from the coast. The study site lies between the aeolian Namibian sand sea in the west and Great Namibian Escarpment in the east (Fig. 1). All necessary permits were obtained for the described study, which complied with all relevant regulations (Permit 1854, Ministry of Environment and Tourism; Permit NRNR/P/2014/01, NamibRand Nature reserve). The reserve soil is red Kalahari sand with vegetation dominated by *Stipagrostis obtusa*, *S. uniplumis*

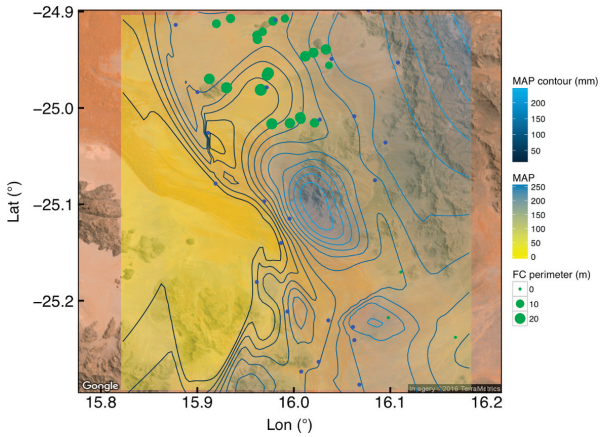

Figure 1. Variation in mean annual precipitation (MAP) average between 2004 and 2014 across the study site superimposed over a Google Earth image of the area. The size of the green points indicates the average lengths of fairy circle perimeters at the locations of soil infiltration measurements (n = 35). The colour and contour lines are derived from bicubic spline interpolation of MAP across the area. Blue points represent the locations of the rainfall gauges. The average MAP for the area (2004–2014) was 113 ± 6.3 mm annum^{-1} (mean ± SE, n = 45).

and *S. ciliata* of the Poaceae. Rain is concentrated in summer, peaking in Feb with 62% falling in Jan–Apr. Herbivores that commonly occur in the grasslands include oryx, zebra, springbok, ostrich, hartebeest.

Measures of the variation in plant biomass, soil CO_2 flux and water and ^{15}N transport (see below) were conducted at a single site within the reserve (24.964°S, 15.974°E). Infiltration measures were carried out across the reserve (Fig. 1) to document the variability of fairy circle size and soils.

Grass canopy volumes and biomass

For each of six pairs of fairy circles (randomly selected) within a single area (24.964°S, 15.974°E), the distance between peripheries was measured and a line stretched taught between peripheries (Fig. 2). Plants were excavated in the periphery at either end of the transect, at 25% (quartile), the mid-point and 75% (quartile) along the transects (Fig. 2). We were careful to recover all the coarse roots of the plants down to a depth of 40 cm, but this misses much of the fine root biomass. From trenches dug alongside peripheral grasses we know that the roots extend to a depth of up to 0.9 m, but coarse roots were only observed on the side-walls of the excavations within 0.4 m of the plants, whereas sparse finer hair-like roots were observed up to ca 0.9 m from the peripheral plant stems in barren circles. The canopy heights, widths and longest root lengths (coarse roots) of the plants were recorded and the plants bagged for biomass measurements. The collected plant material was separated into root and shoot components and dried at 70°C for 96 h prior to weighing. The fragile dried root sheaths were then removed from the roots by crumbling them by hand in a plastic bag. The root material was then re-weighed.

Independent of the transects, grass clump densities on the periphery of circles and in matrix were also measured. For each fairy circle (n = 10) within a single area (24.964°S, 15.974°E) the perimeter of the circle was measured by laying

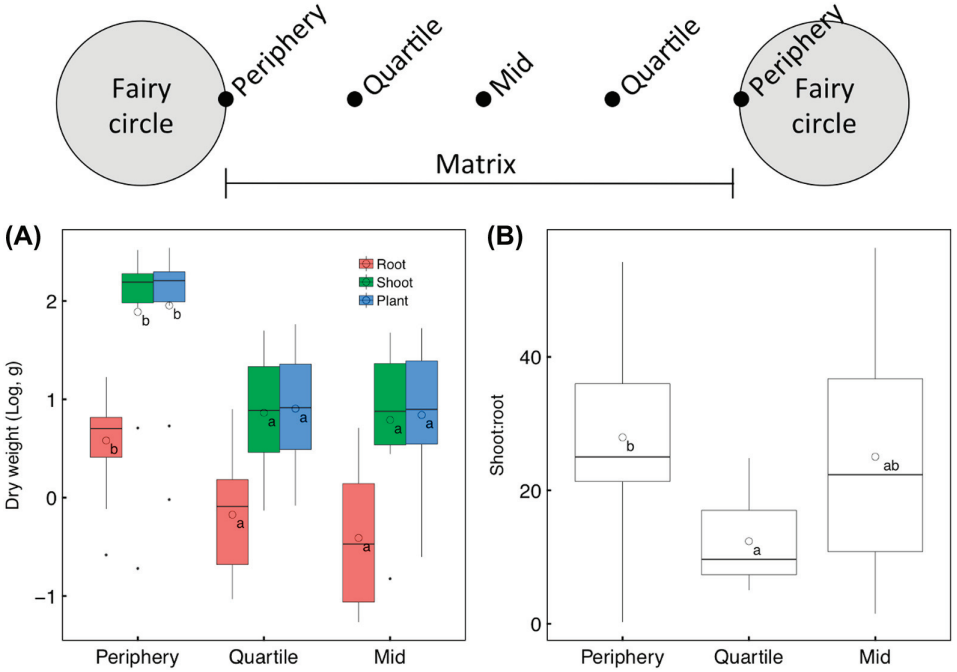

Figure 2. The variation in (A) shoot, root and plant dry biomass and (B) shoot:root biomass ratios between the periphery of fairy circles, the quartile and midpoint of distance (see inset diagram) between neighbouring circles in the matrix (n = 6 transects). The boxes and horizontal lines represent the first and third quartiles and the medians, respectively. The whisker represents 1.5 × the interquartile range and outliers above/below that are shown as closed points. The mean (open circle) is also shown with different letters indicating significant differences determined by one-way ANOVA followed by post-hoc Tukey tests (shoot, roots, plants and shoot:root ratios tested separately).

a tape along the peripheral grass. This line was used to count the number of tussocks on the periphery of each circle. The number of plants in 1 m^2 quadrats (n = 10) in the matrix (equidistant from 2 neighbouring circles) were counted. The heights and canopy widths of 5 plants were measured for each circle and also for each 1 m^2 quadrat to allow estimation of canopy volumes.

Soil CO_2 efflux

Soil respiration was measured as an indicator of soil biotic activity along four independent transects running from the barren interior, through the periphery and into the grassland matrix at the same site at which grass biomass was measured (24.964°S, 15.974°E). A LI-6400 portable infra-red gas analyser (LI-COR Biosciences, NE, USA) with a Licor soil respiration cuvette (Licor 6400-09) was used to measure soil CO_2 efflux between 8 am and 11 am (Feb 2014). The rim of the soil cuvette was inserted 1 cm into the soil and allowed to equilibrate for 5 min prior to conducting soil CO_2 efflux measurements. For each measurement, the soil temperature was measured over a 0 to 20 cm depth with a Licor soil temperature probe (mean 30.5°C). The CO_2 efflux measurements were taken thrice at a cuvette CO_2 concentration of 400 µl l^{-1} over a range of 10 µl l^{-1} and averaged.

Soil infiltration rates and textural analysis

We measured soil water infiltration by taking a single measurement at each of 35 sites across the nature reserve, varying from having no fairy circles to having highly regular densely packed fairy circles (e.g. Supplementary material Appendix 1, Fig. A2). These sites were all close to roads and were chosen to represent the variability of fairy circles across the reserve. Infiltration was measured following the method of Herrick et al. (2005) using a single ring infiltrometer (12.8 cm diameter). Briefly, the soil was wetted with 400 ml of water applied to the surface through a towel, prior to insertion of the infiltrometer into the soil to a depth of 3 cm. The infiltrometer was loaded with 400 ml water using a plastic sheet to reduce soil surface disturbance, and then the reservoir replenished using a Mariotte's bottle (McCarthy 1934) to keep a constant head of pressure. The change in volume over time was recorded and the infiltration rate calculated as in Herrick et al. (2005). At each site a soil sample was taken to 30 cm depth with an auger. By augering deeper, the depth of a calcrete layer was measured if present at < 50 cm depth (depths ranged between 8 and 50 cm).

For each sample collected (n = 35), soil particle size distributions were analysed thrice using a Malvern Mastersizer 2000 (Malvern Instruments, Malvern, UK) on < 1 mm sieved soils suspended in water and ultrasonically dispersed, stirred and introduced to the laser diffractometer with a Malvern Hydro 2000G wet dispersion unit. The organic material that floated to the surface was removed by hand. Each sample was subjected to 180 s ultrasonic dispersal to ensure complete disaggregation of particles. The average proportion of the soil particles in each size class were recorded and plotted. These size classes were then summed into categories representing clay, silt and sand (and sand sub-classes), according to the Wentworth grain size chart (Williams et al. 2006).

A multiple regression model for infiltration rate against soil texture and environmental variables, including mean annual precipitation (MAP) and temperature (MAT) and normalised difference vegetation index (NDVI) and each of their respective quadratic terms, was developed in R (R Development Core Team). The inclusion of MAT, MAP and NDVI were based in the assumption that these may relate to vegetation density and decomposition and thus soil carbon and consequently infiltration rates. The model was simplified though backward simplification following the procedure outlined by Crawley (2007). In this model the soil texture and NDVI variables were logit transformed. The simplified model retained only sand, MAT and MAP.

Environmental data

Monthly rainfall data were obtained from 45 stations within the NamibRand reserve for the period 2004–2014. These data were averaged over the decade and the calculated MAP subject to interpolation across longitude and latitude using cubic splines according to Akima (1978) implemented in the 'akima' package in R. We produced our own interpolated rainfall measures because global interpolated datasets (Hijmans et al. 2005) poorly represent the variation in rainfall across this region due to the highly stochastic nature of rainfall. Mean annual temperatures (MAT) were obtained from Hijmans et al. (2005) for the period 1950–2000 (ca 1 km^2 resolution) using the 'raster' package in R. Normalized difference vegetation index (NDVI) is a measure of the density of chlorophyll contained in vegetative cover. The annual average NDVI were obtained for southern Africa from eMODIS TERRA produced by US Geological Survey Earth Resources Observation and Science Center through time series smoothing (Swets et al. 1999) of data collected between 2001 and 2010 (250 m spatial resolution). These data were sampled for the locations of the infiltrations sites using the 'raster' package in R.

Fairy circle size, shape and density

At each site where infiltration measurements were made and soil samples collected, we traced the outline of fairy circles using the line tool in Google Earth. We checked all available Google Earth imagery for fairy circles at each site and used the clearest image from the period 2010–2012, corresponding to a relatively wetter period, on the basis that changes in fairy circles over such a short period are small to non-existent. All visible circles were delineated in an area of ca 2.25 ha centred on the infiltration site. The lines were converted to polygons and analysed using the 'rgeos' and 'spatstat' packages in R. The fairy circle density, average polygon area, diameter and perimeter and average minimum distance between neighbouring polygons were calculated for each site. The shape index (i.e. compactness, SI) was calculated as a measure of the departure of fairy circle shape from a circular plan, as $SI = \frac{perimeter}{2\sqrt{\pi \times area}}$. Fairy

circle periphery lengths were related to infiltration rate and environmental variables using a multiple regression model in R. This model initially included the infiltration rate, MAT, MAP, logit transformed depth of calcrete layer, logit transformed NDVI, and each of their respective quadratic terms, but backward simplification following the procedure outlined by Crawley (2007) resulted in retention of only infiltration rate and MAP.

Water pulse conduction

At one site (24.964°S, 15.974°E), water 'depots' were created inside a fairy circle and independently in the matrix between fairy circles by depositing a large volume of water in the soil. Water flux from these depots was monitored over a 1 month period. Three circles within a 1 ha area were equipped with Decagon 10HS soil water probes (Decagon Devices, Pullman, WA, USA) buried at 20 and 50 cm depth on 23 Feb 2014. The probes were located in the matrix, periphery and the interior of the fairy circles. To install the probes a hole was augured to below the required depth, the insertion depth marked using a meter rule, and the probe inserted horizontally in the sidewall of the augured hole. The augured hole was then filled with the material taken from the hole (first out, last in). The probes were connected to Decagon Emb5 loggers set to record once every 4 h. On 27 Feb 2014 at 16:00 h 20 l of water was poured into a 9 cm diameter pipe placed in an augured hole extending to 50 cm depth resulting in wetting of the soil from surface. Two independent water depots were established, one in the matrix at 4.5 m from the periphery of a circle and the other in the barren area of a separate fairy circle, 3 m from its periphery. Both water depots were ca 0.5 m from a set of probes at that location.

^{15}N labelling and analyses

At one site (24.964°S, 15.974°E), ^{15}N soil 'depots' were established by introducing a solution containing ^{15}N at varying distances into both the matrix and fairy circle from peripheral grasses and the uptake of ^{15}N by the peripheral grasses monitored. A 20 l solution containing 2.2 g of 98 atom% (i.e. percentage of total N that is ^{15}N) of $^{15}NH_3{}^{15}NO_3$ (Sigma-Aldrich, Johannesburg, South Africa) in water was prepared and 1 l of this poured into a 9 cm diameter pipe inserted into an augured hole to 20 cm depth. These depots of ^{15}N were established in the matrix on 21 Feb 2014 at 1, 2.2 and 4.5 m from the periphery of a circle (n = 5), and within fairy circles 1.5 and 3 m from their periphery (n = 5). A stake marked the peripheral grass clump closest to the ^{15}N-depot. After 7 d (1 Mar 2014), 1 month (19 Mar 2014) and 5 months (8 Jul 2015) the youngest green leaves were harvested from the marked grass clumps. The foliar material was dried in an oven at 70°C for 48 h and then milled in a Wiley mill using a 0.5-mm mesh and subjected to mass spectrometer analysis for leaf δ^{15}N and δ^{13}C values. The milled leaf samples (2.1–2.2 mg) were weighed into tin capsules (Elemental Microanalysis, Devon, UK) and combusted in a Thermo Flash EA 1112 series elemental analyzer and the gasses were fed into a Delta Plus XP isotope ratio mass spectrometer (Thermo Electron Corporation, Milan, Italy). Two in-house standards and one International Atomic Energy Agency standard were used to calibrate the results.

Data available from the Dryad Digital Repository: <http://dx.doi.org/10.5061/dryad.s6c7j> (Cramer et al. 2016).

Results

Evidence of facilitative and competitive dynamics

The height and diameters of *Stipagrostis ciliata* grasses that mostly comprise the fairy circle periphery are much larger than those of the mixture of *S. ciliata*, *S. uniplumis* and *S. obtusa* grasses in the matrix (Table 1). We measured all plants regardless of species, and thus these measures reflect both the species compositional shift and an environmental gradient between periphery and matrix. These heights and diameters translate to more than an order of magnitude difference in plant volume (assuming a cylindrical volume). Although the density of smaller matrix grasses is much higher than that of the peripheral grasses, when combined with the canopy volume estimate this yields a 5-fold larger canopy volume per area on the fairy circles (including the barren area in the estimate) relative to the matrix (Table 1). Across the landscape with an average canopy volume of 24 ± 1 l m^{-2} (i.e. volume per ground area), the canopy volume was 3.2-fold greater on the fairy circles than in the landscape as a whole.

The whole-plant dry weights of peripheral grasses were ca 10-fold greater than those at the quartile (25%) and midpoints of the inter-fairy circle distance between neighbours

Table 1. Plant canopy characteristics measured on fairy circle peripheries (n = 10), in the matrix (n = 10) and an average for the landscape (i.e. including fairy circles and matrix). Individual plant heights and canopy diameters (n = 5 per area) were used to calculate plant canopy volume, and using plant density, this was expressed on the basis of area. Plant density and canopy volume per area for the entire landscape were estimated using area-weighted averages based on the landscape occupancy of fairy circles (14.7%) for this site. Values are mean ± SE.

Measure	Fairy circle	Matrix	Landscape
Height (m)	0.36 ± 0.01	0.13 ± 0.01	0.25 ± 0.01
Diameter (m)	0.40 ± 0.01	0.08 ± 0.01	0.24 ± 0.01
Canopy volume (L)	46 ± 4	0.9 ± 0.2	24 ± 2
Plant density (# m^{-2})	1.6 ± 0.1	24.6 ± 3.7	21.2 ± 3.2
Canopy volume per area (l m^{-2})	75 ± 7	15 ± 2	24 ± 1
Canopy volume relative to landscape	3.17 ± 0.29	0.63 ± 0.05	

(Fig. 2, note $\log_{10}$ scale). The shoot:root ratios of all of the grasses were high, possibly because it was not possible to recover all of the roots and because the grass tufts contain moribund biomass. These results, however, reliably represent the root mass in the surface 40 cm of soil, with the sand sheath removed. The shoot:root ratios of the peripheral grasses were highest and those at the quartile distances lowest, while the mid-point grass shoot:root ratios were intermediate between periphery and quartile distances. The depth of the coarse roots of the peripheral grasses were 32.7 ± 2.6 cm while that of the matrix grass at the quartile distance was 23.6 ± 0.6 cm and at the midpoint 20.8 ± 1.1 cm ($n = 6$), consistent with the variation in root biomass (Fig. 2).

Soil CO_2 and H_2O efflux

Soil CO_2 and H_2O efflux (i.e. evaporation) was low at all points across the transects, despite 10 mm of rainfall one week prior to the measurements (Fig. 3). The CO_2 and H_2O efflux were undetectable at the centre of the circles (no data obtained), and very low at points further than 1 m from the periphery. The CO_2 efflux in the matrix was ca 50% of that on the periphery, broadly consistent with the lower root mass of matrix than peripheral grasses (Fig. 2). Water efflux was also highest at the periphery and lowest in the centre of the fairy circle.

Fairy circle size and shape

Fairy circles are not actually circular when closely inspected (Supplementary material Appendix 1, Fig. A2). The lack of circularity is due to convoluted perimeters, but not to elongation in any particular direction. The shape index (SI) of fairy circles is 1.152 ± 0.014 ($n = 29$ sites), indicating a 15% greater perimeter length than that expected for a circular structure of equivalent area. The peripheral length of the fairy circles was thus used as an estimate of the amount of peripheral grass and the size of fairy circles. At the site where we measured canopy volumes and investigated ^{15}N transfer between fairy circles and water fluxes (24.964°S, 15.974°E), SI is 1.140 ± 0.011 ($n = 151$ fairy circles). At this site fairy circle landscape occupancy is 14.7% with 30.8 circles ha^{-1} and the average fairy circle area is 40.0 ± 1.6 m^2 with a diameter of 6.9 ± 0.14 m and a perimeter of 25.1 ± 0.7 m. These circles are 5.7 ± 0.2 m apart (representing the average minimum distance between the peripheries of neighbouring circles) and 12.9 ± 0.3 m apart (centroid to centroid).

Fairy circle morphology related to soil infiltration rates

Soil infiltration measures were all conducted within a geographic area (range = 72 km) in which fairy circles do occur (Fig. 1). Infiltration rates were ubiquitously high (Fig. 4A), exceeding the normal range (i.e. > 126 mm h^{-1}) for a variety of soils in the USA (Johnson 1963). Fairy circle peripheral lengths were positively related to soil infiltration rates. There was, however, a broad scatter of points between the 5% and 95% quantile regression lines, indicating that the dependence was likely influenced by other variables. A multiple regression model predicted 60.7% of fairy circle peripheral lengths (Fig. 4B) based on infiltration rate and MAP, with the logit transforms of calcrete layer depth and NDVI having been dropped during simplification.

Within the geographic area, sites with fairy circles within ca 75 m of the soil sample had significantly greater proportion of coarse particles (> 300 μm) and correspondingly smaller proportions of fine particles (< 30 μm; Supplementary material Appendix 1, Fig. A3). This resulted in significantly more sand and correspondingly less silt and clay at sites with fairy circles than at sites without fairy circles (Supplementary material Appendix 1, Table A1). Soil

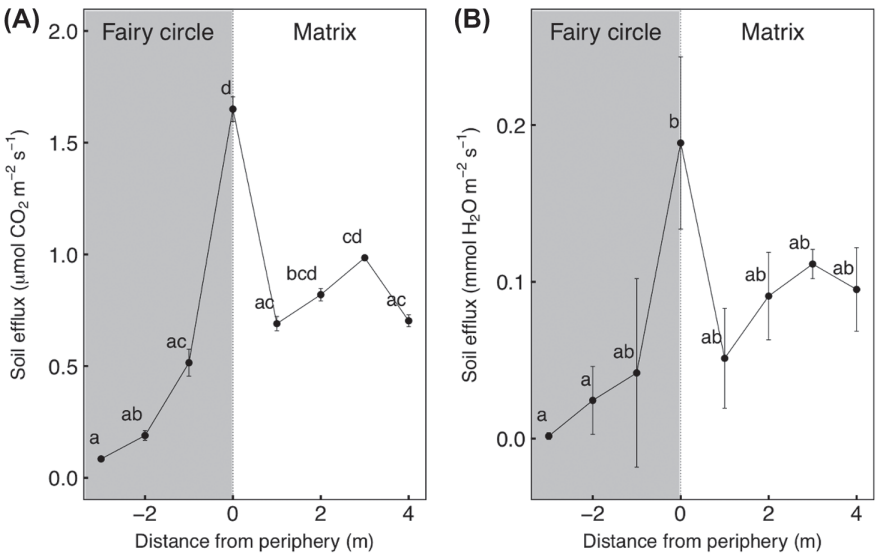

Figure 3. Variation in soil (A) CO_2 and (B) H_2O efflux with position along transects ($n = 4$ transects) from the barren area inside a fairy circle (grey panel, negative distances from periphery) into the matrix (clear panel, positive distances from periphery). Points represent mean and bars SE. Different letters indicate significant differences determined by one-way ANOVA followed by post-hoc Tukey tests.

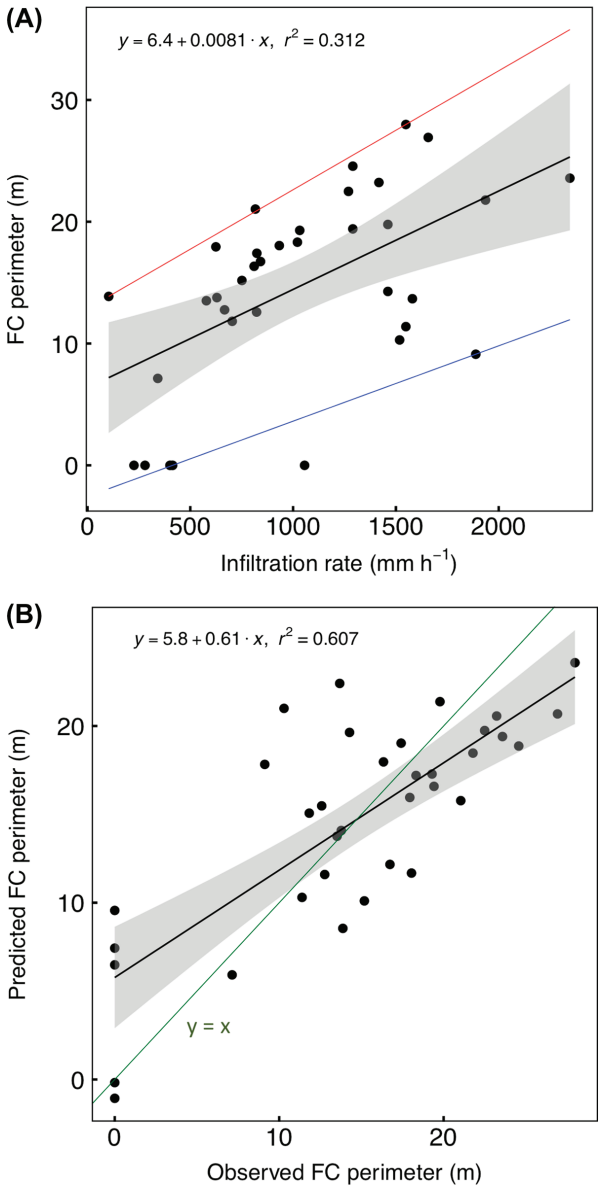

Figure 4. (A) Variation in fairy circle (FC) perimeter lengths averaged across fairy circles with soil infiltration rate at each of 35 sites. The red, black and blue lines represent the significant 95%, 50% and 5% quantile regression lines and the grey band represents the 95% confidence limit. (B) Correspondence of multi-linear regression prediction of fairy circle perimeter with observed perimeters. The grey band represents the 95% confidence limit on the prediction (black line) and the green line represents $y = x$. The equation and r^2 are for the best-fit line. The multiple regression equation was: FC perimeter = $-17.1 + 0.023 \bullet Inf - 7.38 \times 10^{-6} \bullet Inf^2 - 0.16 \bullet MAP + 0.33 \times 10^{-6} \bullet MAP^2$ (Inf = infiltration rate; MAP = mean annual precipitation; $p < 0.01$ for all terms).

infiltration rates were strongly related to the texture of the soil, with 52% of variance in infiltration rate explained by soil texture, MAT and MAP (Table 2). The proportion of sand in the soil had a particularly strong positive relationship with infiltration rate (Supplementary material Appendix 1, Fig. A4), suggesting that sandy soils enable high hydraulic conductivity.

Table 2. Multiple regression analysis of the predictors of infiltration rate. The predictors listed were retained in the model after backward simplification based on AIC scores. Predictor variables that were collinear ($r > 0.7$) with sand were not included (clay and silt). The initial model included all linear and quadratic terms for the variables listed as well as NDVI. The coefficients for the multiple regression and the standardized Beta coefficients are shown for each predictor. The proportion of sand in the soil was logit transformed prior to analysis. The final model had an adjusted r^2 value of 0.52 ($p < 0.001$).

Predictor	Coefficient	SE	Beta	p
Intercept	6281	1787		
Sand	498	95	0.63	< 0.001
MAT	–22	9	–0.29	0.024
MAP	–31	12	–0.32	0.012

Soil conduction of water pulses

The capacity of the soils to rapidly transport water over long distance (ca 7.5 m) was demonstrated by injection of water pulses followed by tracking soil moisture at sites remote from the pulse (Fig. 5). There was a strong diurnal fluctuation in soil water content registered at all probes and depths that was only temporarily suppressed at the probe closest to the pulse of water (Fig. 5). Addition of water to a site in the matrix was registered as a pulse change in soil water by a water probe at 20 cm depth closest to the site of introduction within hours of the introduction. Within 4 d the probes located on the fairy circle periphery 4.5 m from the water pulse and those within the fairy circle 6 m and 7.5 m from the pulse all registered an increase in soil water content. Similarly, 4 d after the pulse of water was applied in the centre of a fairy circle a change in soil water content was detected 1.5 m from pulse (closer to the periphery), 3 m from pulse (on the periphery) and 5.2 and 7.5 m from the pulse (in the matrix). The probes in the matrix located at 2.2 m from the matrix-pulse and 5.2 m from the fairy circle-pulse, which were both in a location similar to the quartile position (Fig. 2), registered either a small or no change in soil water content. We speculate that these probes were in a soil zone with low soil water content as a consequence of vegetation demand, and/or not in hydraulic contact with the remainder of the soil. Probes at 50 cm depth recorded only small changes in soil water in response to the pulse, except for the probe closest to the pulse (data not shown).

^{15}N uptake by periphery grasses

^{15}N tracers supplied at varying distances from the fairy circle peripheries were detected within peripheral grass foliar tissue within 7 d of application (Fig. 6). The foliar $\delta^{15}N$ values of peripheral grasses remote from the ^{15}N injection point ('control') were confined to relatively narrow limits and varied little between repeated samplings (7 d, 1 and 5 months). ^{15}N depots located 1 m from peripheral grasses resulted in considerable increases in $\delta^{15}N$ within 7 d, and this signal persisted to the 5-month sampling, which took place in the middle of the dry winter period. Likewise, there was significant enrichment of the peripheral foliar $\delta^{15}N$ from ^{15}N placed 2.25 and 4.5 m into the matrix, demonstrating transfer of the isotope to the peripheral grass. There was also enrichment from ^{15}N

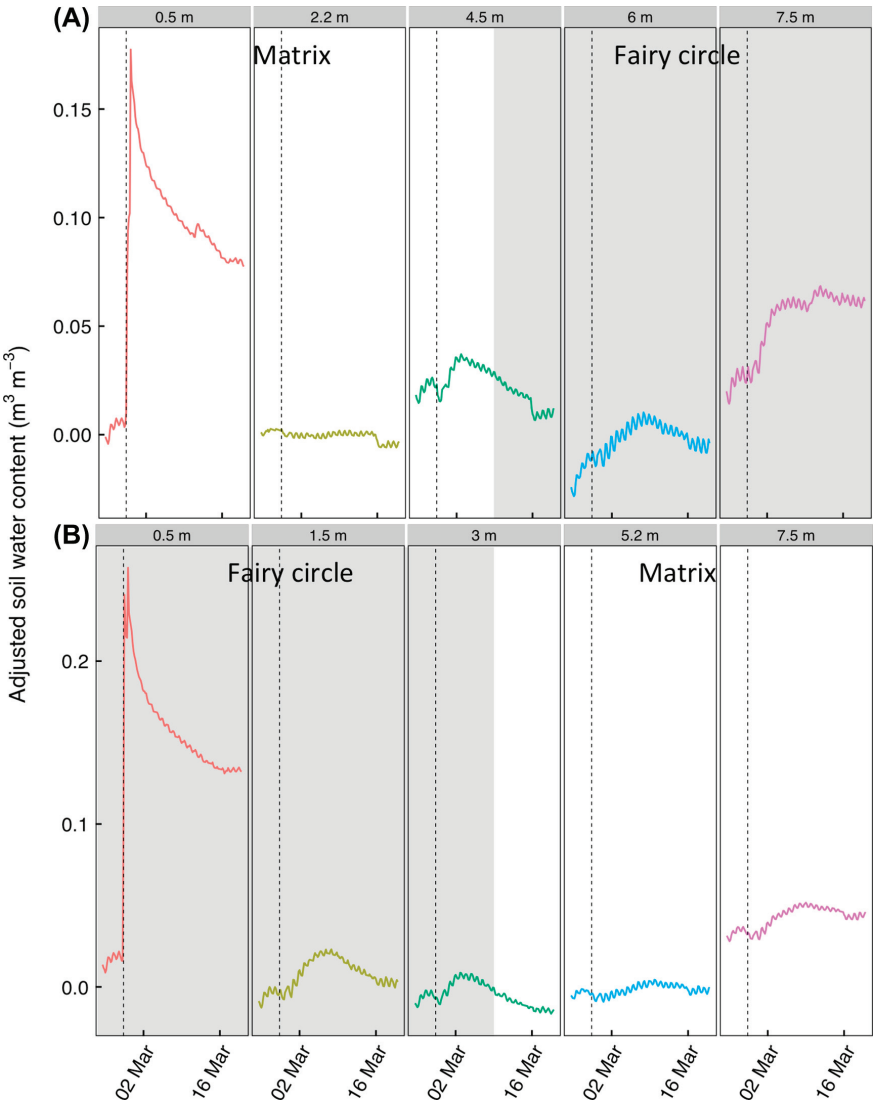

Figure 5. Soil moisture content changes at 20 cm depth in response to a pulse of water (A) in the matrix 4.5 m from periphery and (B) in the centre of a fairy circle 3 m from periphery. The grey bands represent the approximate extent of the fairy circle. Soil moisture content was adjusted for variation in water content of control measurements made in a nearby circle where no pulse was supplied. The broken vertical line indicates the time when the pulse was delivered.

depots placed in the fairy circles at 1.5 and 3 m from the periphery. When the injection point was in the fairy circles, the $\delta^{15}N$ values of the peripheral grasses had a number of outliers, some with very high $\delta^{15}N$ values.

Discussion

The variation in vegetation biomass and shoot:root allocation between the fairy circle periphery and matrix provides evidence for either or both facilitation (between peripheral grasses) and competitive interactions (i.e. between periphery and barren areas of fairy circles and between periphery and matrix). This variability in biomass (over tens of metres; Getzin et al. 2015a, b) occurs despite dense fairy circles at the study site occurring in an extremely homogenous (i.e. both between fairy circles and matrix and at the landscape scale) edaphic environment that mostly comprises deep aeolian sands (Cramer and Barger 2013). The relationship between soil infiltration rates and fairy circle size indicates an association of fairy circles with soil properties that are conducive to long-range (several metres) hydraulic and nutrient transfer. The capacity for these transfers was demonstrated by both water and $^{15}NH_3{}^{15}NO_3$ mobility within the soil. These data are consistent with the vegetation-patterning hypothesis of fairy circle origins, and establish that the conditions required for this mechanism of formation are present at a site where fairy circles occur. This does not, however, represent a test of the formation mechanism.

Peripheral grasses are commonly larger than matrix grasses, although this is not necessarily the case for all fairy circles (Tschinkel 2012). In some circumstances this size differential is associated with different species, but in others the same species occurs on the periphery as on the matrix. The peripheral grass canopy volume was considerably greater (3.17-fold, Table 1) than the average for the landscape. The

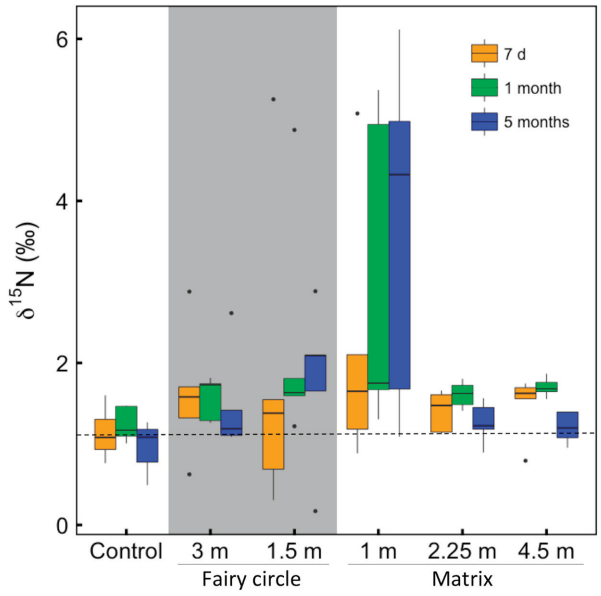

Figure 6. The variation in peripheral grass foliar $\delta^{15}N$ values sampled 7 d, 1 and 5 months after supply on 21 Feb 2014. The ^{15}N isotope was supplied at varying distances from the peripheral grasses, either in the matrix (1, 2.25 and 4.5 m) or in the fairy circles (1.5 and 3 m, represented by grey band). The boxes and horizontal lines represent the first and third quartiles and the medians, respectively. The whisker represents 1.5 × the interquartile range and outliers above/below are shown as points. The horizontal broken line represents the overall median of the control samples.

ca 10-fold higher total biomass of plants on the periphery than at the quartile location in matrix was also associated with significantly higher (2.3-fold) shoot:root ratios. Since light competition is unlikely in this high-light environment with extremely sparse grass canopies, higher biomass and shoot:root ratios on the periphery may represent a response to a less stressful environment (Chapin 1980) generated through a lack of competition from the interior of the barren fairy circles. In contrast, competitive interactions in the matrix may require greater root investment for survival than on the periphery. For example, increased allocation to rooting systems in response to water limitation enables greater access to water (Robinson et al. 2010). Thus the variation in grass biomass and shoot:root ratios between periphery and matrix are consistent with competitive interactions, particularly between the periphery and the adjacent matrix grasses.

The greater biomass of the peripheral grasses may also be considered a consequence of short-range facilitation. In dryland spatial vegetation patterning, facilitation is commonly caused by interception of surface runoff, soil water diffusion or sediment deposition to vegetation clumps (Meron 2012, Zelnik et al. 2015). In the case of Namibian fairy circles, however, competitive exclusion of grasses from the centre of the fairy circle likely allows the peripheral grasses to grow larger through maintenance of a resource (i.e. water and nutrient) reservoir. Once a fairy circle has formed, it may be rare that environmental conditions are sufficiently favourable for grasses to be able to invade the barren fairy circles. Although grass seedlings do commonly establish within the barren area of fairy circles following rains, they rarely survive the following dry period. Thus individual peripheral grasses may benefit from cooperative exclusion of competitive grasses from the barren fairy circle and focussing of resources from the fairy circle into the peripheral band through water and nutrient diffusion powered by grass consumption (Zelnik et al. 2015). Resources flowing outwards from the barren fairy circle are likely to be largely intercepted by the deep-rooted peripheral grasses, resulting in matrix grasses adjacent to the peripheral grasses experiencing intense competition.

As demonstrated by water- and ^{15}N-pulses, resources from both the barren fairy circle and the matrix area meet the water and nutrient requirements of the larger peripheral grasses. The demand of these larger peripheral grasses likely dominates resource fluxes in the landscape due to the concentration of plant biomass on the fairy circle periphery (Table 1). Furthermore, it has been commonly shown that larger deep-rooted species, including grasses, engage in hydraulic redistribution (i.e. lift) of water into surface soils (Leffler et al. 2005). Hydraulic redistribution by peripheral grasses is likely to contribute to growth on the periphery and may also contribute to explaining the greater surface flux of water from the periphery (Fig. 3B) where root biomass was focused, as evident from both plant biomass (Fig. 2) and CO_2 fluxes (Fig. 3A). The sparse canopy of the grasses, including those on the periphery, thus does not serve to reduce evaporation from the soil. This is in contrast to the reduced evaporative flux of water from soil under the peripheral vegetation of a gap pattern in a shrubland in Niger (Barbier et al. 2008). Thus the concentration of biomass on the fairy circle periphery results in the peripheral grass functioning as a sink for resources from the fairy circle and also from the matrix, potentially resulting in competition between neighbouring fairy circles for resources and consequently the regular spacing of fairy circles documented by Getzin et al. (2015a, b).

Since grass root lengths and radial extents are relatively restricted (< 1 m; Juergens 2013) and surface runoff is rare (Cramer and Barger 2013), competitive interactions over distances greater than 1 m requires resource mobility in the soil. The exceedingly high infiltration rate in sites with fairy circles relative to global norms indicates high capacity for hydraulic transfer in the soil. This is also demonstrated by the water-pulse experiments that show water movement over distances of up to 7.5 m over days to weeks. The transfer of ^{15}N to peripheral grasses within 7 d over distances of 3 m from inside a fairy circle and 4.5 m from the matrix (Fig. 6) additionally indicates significant capacity for mobility of N through the sand. This mobility of N is probably powered by water flux through soils with very low clay and carbon contents, and thus binding capacity for nutrients. Since the fairy circles are, on average, at least 5.7 m apart at the study site used for water and ^{15}N depot experiments, the capacity for water and N movement to the periphery from the matrix over these distances indicates that the fairy circles and the matrix in the vicinity of fairy circles are hydraulically and nutritionally connected.

The positive association of fairy circle perimeter lengths (as a measure of fairy circle size) with soil infiltration rates indicates that regionally, fairy circles are larger when the infiltration rates are higher, but decreases with increasing MAP. Fairy circle occurrence in south-western Africa (including Namibia) was previously also negatively related to

MAP (Cramer and Barger 2013). The main determinant of infiltration rate is the proportion of the soil that is the sand content, which allows the development of larger fairy circle perimeters in low rainfall areas. The association of fairy circle size with infiltration rates is consistent with the requirement of vegetation-patterning that neighbouring fairy circles interact with each other in order for them to attain highly regular patterning (Getzin et al. 2015a, b). High soil water conductivity was also identified as a crucial component in a model of fairy circle formation (Zelnik et al. 2015).

Conclusion

Namibian fairy circles occur in an arid context on soils with exceedingly high infiltration rates and low nutrient holding capacities. We conclude that Namibian fairy circles are an example of an emergent vegetation spatial pattern that arises from soil hydraulic and nutritional characteristics that enable relatively long-range (several metres) resource transport within the soil, rather than from the particular grass species that form the circles, or the flora and fauna that inhabit the circles. This soil-hydraulic mechanism is not the only mechanism forming such vegetation gap-patterns, which also occur in shrublands due to differential soil surface evaporation (Niger; Barbier et al. 2008) and in grasslands due to surface runoff (Australia; Getzin et al. 2016).

Acknowledgements – We are grateful for funding from National Geographic Grant #9539-14 to Nichole Barger. We are grateful to Quintin and Vanessa Hartung, Nils Odendaal and other staff at the NamibRand Nature reserve for accommodating and enabling this research. Nicholas Hanley and Edward Chirwa provided technical assistance and mass spectrometer analysis was conducted by Ian Newton in the Dept of Archeometry (Univ. of Cape Town).

References

Aguiar, M. R. and Sala, O. E. 1999. Patch structure, dynamics and implications for the functioning of arid ecosystems. – Trends Ecol. Evol. 14: 273–277.

Akima, H. 1978. A method of bivariate interpolation and smooth surface fitting for irregularly distributed data points. – ACM T. Math. Softw. 4: 148–159.

Barbier, N. et al. 2006. Self-organized vegetation patterning as a fingerprint of climate and human impact on semi-arid ecosystems. – J. Ecol. 94: 537–547.

Barbier, N. et al. 2008. Spatial decoupling of facilitation and competition at the origin of gapped vegetation patterns. – Ecology 89: 1521–1531.

Borgogno, F. et al. 2009. Mathematical models of vegetation pattern formation in ecohydrology. – Rev. Geophys. 47: RG 1005.

Brouwer, C. et al. 1988. Irrigation water management: training manual no 5. – Food and Agriculture Organization of the United Nations, Rome, <www.fao.org/docrep/s8684e/s8684e0a.htm>.

Chapin, S. F. I. 1980. The mineral nutrition of wild plants. – Annu. Rev. Ecol. Syst. 11: 233–260.

Couteron, P. and Lejeune, O. 2001. Periodic spotted patterns in semi-arid vegetation explained by a propagation-inhibition model. – J. Ecol. 89: 616–628.

Cramer, M. D. and Barger, N. N. 2013. Are Namibian 'fairy circles' the consequence of self-organizing spatial vegetation patterning? – PLoS One 8: e70876.

Cramer, M. D. et al. 2009. The importance of nutritional regulation of plant water flux. – Oecologia 161: 15–24.

Cramer, M. D. et al. 2016. Data from: Edaphic properties enable facilitative and competitive interactions resulting in fairy circle formation. – Dryad Digital Repository, <http://dx.doi.org/10.5061/dryad.s6c7j>.

Crawley, M. J. 2007. The R book. – Wiley and Sons.

Deblauwe, V. et al. 2008. The global biogeography of semi-arid periodic vegetation patterns. – Global Ecol. Biogeogr. 17: 715–723.

Deblauwe, V. et al. 2011. Environmental modulation of self-organized periodic vegetation patterns in Sudan. – Ecography 34: 990–1001.

Eldridge, D. J. et al. 2000. Infiltration through three contrasting biological soil crusts in patterned landscapes in the Negev, Israel. – Catena 40: 323–336.

Fernandez-Oto, C. et al. 2014. Strong interaction between plants induces circular barren patches: fairy circles. – Phil. Trans. R. Soc. A 372: 20140009.

Getzin, S. et al. 2015a. Clarifying misunderstandings regarding vegetation self-organisation and spatial patterns of fairy circles in Namibia: a response to recent termite hypotheses. – Ecol. Entomol. 40: 669–675.

Getzin, S. et al. 2015b. Adopting a spatially explicit perspective to study the mysterious fairy circles of Namibia. – Ecography 38: 1–11.

Getzin, S. et al. 2016. Discovery of fairy circles in Australia supports self-organization theory. – Proc. Natl Acad. Sci. USA 113: 201522130.

Herrick, J. et al. 2005. Monitoring manual for grasslands, shrubland and savanna ecosystems. – Volume I and II, Jornada Experimental Range, USDA, NM, USA.

Hijmans, R. J. et al. 2005. Very high resolution interpolated climate surfaces for global land areas. – Int. J. Climatol. 25: 1965–1978.

Johnson, A. I. 1963. A field method for measurement of infiltration. – Washington, Geological Survey Water-Supply Paper 1544-F, United States Government Printing Office, 27.

Juergens, N. 2013. The biological underpinnings of Namib Desert fairy circles. – Science 339: 1618–1621.

Juergens, N. 2015. Exploring common ground for different hypotheses on Namib fairy circles. – Ecography 38: 12–14.

Juergens, N. et al. 2015. Weaknesses in the plant competition hypothesis for fairy circle formation and evidence supporting the sand termite hypothesis. – Ecol. Entomol. 40: 661–668.

Leffler, A. J. et al. 2005. Hydraulic redistribution through the root systems of senesced plants. – Ecology 86: 633–642.

Lejeune, O. et al. 1999. Short range co-operativity competing with long range inhibition explains vegetation patterns. – Acta Oecol. 20: 171–183.

Lyford, F. P. and Qashu, H. K. 1969. Infiltration rates as affected by desert vegetation. – Water Resour. Res. 5: 1373–1376.

McCarthy, E. L. 1934. Mariotte's bottle. – Science 80: 100.

Meron, E. 2012. Pattern-formation approach to modelling spatially extended ecosystems. – Ecol. Model. 234: 70–82.

Moll, E. J. 1994. The origin and distribution of fairy rings in Namibia. – In: Seyani, J. H. and Chikuni, A. C. (eds), Proceedings of the 13th Plenary Meeting AETFAT, Malawi, pp. 1203–1209.

Rietkerk, M. and van de Koppel, J. 2008. Regular pattern formation in real ecosystems. – Trends Ecol. Evol. 23: 169–175.

Rietkerk, M. et al. 2000. Multiscale soil and vegetation patchiness along a gradient of herbivore impact in a semi-arid grazing system in west Africa. – Plant Ecol. 148: 207–224.

Rietkerk, M. et al. 2002. Self-organization of vegetation in arid ecosystems. – Am. Nat. 160: 524–530.
Robinson, D. et al. 2010. Root-shoot growth responses during interspecific competition quantified using allometric modelling. – Ann. Bot. 106: 921–926.
Swets, D. L. et al. 1999. A weighted least-squares approach to temporal NDVI smoothing. – Proceedings of 1999 ASPRS Annual Conference: From Image to Information, Portland, Oregon, 17–21 May 1999. American Society for Photogrammetry and Remote Sensing, pp. 526–536.
Tlidi, M. et al. 2008. On vegetation clustering, localized bare soil spots and fairy circles. – Lect. Notes Phys. 751: 381–402.
Tschinkel, W. R. 2012. The life cycle and life span of Namibian fairy circles. – PLoS One 7: e38056.
Tschinkel, W. R. 2015. Experiments testing the causes of Namibian fairy circles. – PLoS One 10: e0140099.
van Rooyen, M. W. et al. 2004. Mysterious circles in the Namib Desert: review of hypotheses on their origin. – J. Arid Environ. 57: 467–485.
Vlieghe, K. et al. 2015. Herbivory by subterranean termite colonies and the development of fairy circles in SW Namibia. – Ecol. Entomol. 40: 42–49.
Williams, S. J et al. 2006. Surficial sediment character of the Louisiana offshore Continental Shelf region: a GIS compilation. – U.S. Geological Survey Open-File Report 2006-1195, <http://pubs.usgs.gov/of/2006/1195/index.htm>.
Zelnik, Y. R. et al. 2015. Gradual regime shifts in fairy circles. – Proc. Natl Acad. Sci. USA 112: 12327–12331.

Supplementary material (Appendix ECOG-02461 at <www.ecography.org/appendix/ecog-02461>). Appendix 1.